The Substrate Binding Site of Human Liver Cytochrome P450 2C9: An NMR Study†

Sonia Poli-Scaife, Roger Attias, Patrick M. Dansette, and Daniel Mansuy*

Laboratoire de Chimie et Biochimie Pharmacologiques et Toxicologiques, URA 400 CNRS, Université Paris V, 45 Rue des Saints-Pères, 75270 Paris Cedex 06, France

Received March 6, 1997; Revised Manuscript Received June 19, 1997⊗

ABSTRACT: Purified recombinant human liver cytochrome P450 2C9 was produced, from expression of the corresponding cDNA in yeast, in quantities large enough for UV−visible and ^{1}H NMR experiments. Its interaction with several substrates (tienilic acid and two derivatives, lauric acid and diclofenac) and with a specific inhibitor, sulfaphenazole, was studied by UV−visible and ^{1}H NMR spectroscopy. At 27 °C, all those substrates led to an almost complete conversion of CYP 2C9 to high-spin ($S = {}^5/_2$) CYP 2C9−substrate complexes characterized by a Soret peak at 390 nm; their K_D values varied between 1 and 42 μM. On the contrary, sulfaphenazole led to a low-spin ($S = {}^1/_2$) CYP 2C9 complex upon binding of its NH_2 group to CYP 2C9 iron. Interactions of the five substrates with the enzyme were studied by paramagnetic relaxation effects of CYP 2C9−iron(III) on the ^{1}H NMR spectrum of each substrate. Distances between the heme iron atom and substrate protons were calculated from the NMR data, and the orientation of the substrate relative to iron was determined from those distances. Finally, a model for substrate positioning in the CYP 2C9 active site was constructed by molecular modeling studies under the constraint of the iron−proton distances. It points out two structural characteristics for a compound to be selectively recognized by CYP 2C9: (i) the presence of an anionic site able to establish an ionic bond with a putative cationic residue of the protein and (ii) the presence of an hydrophobic zone between the substrate hydroxylation site and the anionic site. Sulfaphenazole was easily included in that model; its very high affinity for CYP 2C9 is due to a third structural feature, the presence of its NH_2 function which binds to CYP 2C9 iron.

Cytochromes P450 constitute a multigene family involving more than 500 members identified so far (Nelson et al., 1996). Some of them play a key role in the metabolism of exogenous compounds such as drugs. Their broad substrate specificity is now well understood in terms of enzyme multiplicity (Gonzalez, 1989). P450s of the 3A and 2C subfamilies are the major isozymes present in human liver (Guengerich & Turvy, 1991). Genetic analysis of the CYP[1] 2C subfamily indicates the presence of at least seven genes with several allelic variants. From the main members of this subfamily known so far, namely, CYP 2C8, 2C9, 2C18, and 2C19, CYP 2C9 seems to be the isozyme expressed at the highest level in human liver (Ged et al., 1988; Romkes et al., 1991; Goldstein et al., 1994). CYP 2C9 is involved in the metabolism in man of many drugs including several nonsteroidal antiinflammatory agents, such as diclofenac, ibuprofen, suprofen, or tenoxicam, as well as other compounds, such as tienilic acid (TA), warfarin, and phenytoin (Goldstein et al., 1994; Mancy et al., 1995).

In order to predict which P450 will be involved in the metabolism of a new biologically active molecule and to understand the structural basis which governs the specificity of a given P450 for a particular drug, it is important to determine the structure of the substrate binding sites of the main human liver P450s. In the absence of crystal structures for such membrane-bound mammalian P450s, the use of a series of indirect methods, combining biochemical results, spectroscopic studies, and theoretical models, is required. This has been done for CYP 2D6 [see, for instance, Modi et al. (1996) and references cited therein]. In the case of CYP 2C9, a model for the interaction of this cytochrome with its substrates has been proposed on the basis of biochemical and UV−visible spectroscopy experiments and molecular modeling (Mancy et al., 1995). In that model, CYP 2C9 substrates, which most often are anionic at pH 7.4, interact through their anionic site with a cationic residue of the protein [for other models, see also Jones, B. C., et al. (1996) and Jones, J. P., et al. (1996)]. This model only gives an idea of the "pharmacophore" recognized by CYP 2C9, corresponding to an envelope of substrates which all exhibit an anionic site about 8 Å distant from their site of hydroxylation by CYP 2C9. The second step toward a 3D model of CYP 2C9−substrate complexes would be to position this envelope of substrates with respect to some components of CYP 2C9 active site. The nature and position of the putative cationic site of the protein, which would play a role in substrate positioning, are not known so far. Therefore, it would be important to determine the position of substrates relative to the CYP 2C9 iron. For that purpose

† This work was supported by a grant from the Ministère de la Recherche et de la Technologie and Rhône-Poulenc (Programme Bioavenir) and fellowships to S.P.-S. from Rhône-Poulenc and the European Community (Biotech Program, BIO 2-CT92-0316).

* To whom correspondence should be addressed. FAX: 33-01-42 86 83 87.

⊗ Abstract published in *Advance ACS Abstracts,* September 15, 1997.

[1] Abbreviations: CYP, cytochrome P450; 3D, three dimensional; ^{1}H NMR, proton nuclear magnetic resonance; SDS−PAGE, sodium dodecyl sulfate−polyacrylamide gel electrophoresis; *S*, total electron spin; DLPC, dilauroylphosphatidylcholine; TA, tienilic acid; TAI, tienilic acid isomer; DICLO, diclofenac.

S0006-2960(97)00527-8 CCC: $14.00

^{1}H NMR appeared as a powerful and attractive technique, since measurements of paramagnetic relaxation have been successfully used to determine distances between the heme iron and protons of the bound substrate in P450−substrate complexes (Novak et al., 1982; Van de Straat et al., 1987; Woldman et al., 1993; Koerts et al., 1995; Modi et al., 1995, 1996). This was possible because of the high paramagnetism of high-spin iron ($S = 5/2$) in P450−substrate complexes. However, it is noteworthy that ^{1}H relaxation time spectroscopy has not been applied to human P450s as extensively as other spectroscopic techniques because it requires large amounts of highly purified enzymes and sufficiently water-soluble substrates. Quite recently, it was used to study the interaction between CYP 2D6 and codeine (Modi et al., 1996).

This paper reports ^{1}H NMR results about the interaction of a series of substrates with purified CYP 2C9 obtained by expression of the corresponding cDNA in yeast. Starting from iron−substrate proton distances determined in this study, a model for the positioning of substrates in CYP 2C9 active site is proposed. This model takes into account the major interactions that have been recently found to explain the highly specific inhibitory effects of sulfaphenazole toward CYP 2C9 (Mancy et al., 1996).

MATERIALS AND METHODS

All chemicals used were of the highest grade commercially available. Octyl-Sepharose 4B and Sephadex G-25 were purchased from Pharmacia, Biotech AB (Uppsala, Sweden), hydroxyapatite was from Calbiochem-Novabiochem Corp. (La Jolla, CA), DEAE-Trisacryl M was from IBF Biotechnics (Villeneuve la Garenne, France), and Chelex 100 was from Bio-Rad Laboratories (Richmond, VA). Sodium cholate and deoxycholate were purchased from Serva Feinbiochemica Gmbh & Co. (Heidelberg, Germany), lubrol was from Sigma Chemicals (St. Louis, MO), and Triton X-100 was from Fluka Chemie (Buchs, Switzerland). Adenosine 2′,5′-diphosphate, agarose, 2′-AMP, dilauroylphosphatidylcholine (DLPC), diclofenac, lauric acid, piroxicam, and tenoxicam were all from Sigma. Tienilic acid (TA) and its isomer were provided by Anphar-Rolland Laboratories (Chilly-Mazarin, France), and sulfaphenazole was provided by Ciba-Geigy (Basel, Switzerland). [^{14}C]TA (label in the keto group, 43 mCi/mmol) was prepared by CEA (Saclay, France); its radiochemical purity was checked by HPLC and found to be higher than 98%. 2,3-Dichloro-4-(2-thenoyl)phenol (called tienilic acid phenol in the following) was prepared by a previously described procedure (Neau et al., 1990). Deuterated solvents (D_2O, DCl, NaOD) were obtained from SDS (Peypin, France). D_2O purity was never less than 99.8%.

Preparation of CYP 2C9 and NADPH−Cytochrome P450 Reductase. Recombinant CYP 2C9 was produced by expression of the previously reported cDNA (MP-4 clone; Umbenhauer et al., 1987) in the yeast strain W(R) fur1 (Truan et al., 1993) in which cytochrome P450 reductase was overexpressed. Transformation by a pYe DP60 vector containing CYP 2C9 cDNA was performed according to a previously described method (Urban et al., 1994). Yeast culture and microsomes preparations were performed by using described techniques (Bellamine et al., 1994). Microsomes were homogenized in 50 mM Tris-HCl buffer (pH 7.4) containing 1 mM EDTA and 20% glycerol (v/v), aliquoted, frozen under liquid N_2, and stored at −80 °C. P450 contents of yeast microsomes were 130 pmol of P450/mg of protein.

Homogeneous CYP2C9 was purified by a modification of a previously described procedure (Imai, 1976; Beaune et al., 1979) using an octyl-Sepharose column instead of the aminooctyl-Sepharose column. In brief, 15 mL of yeast microsomes (5.5 nmol of P450/mL; 130 pmol of P450/mg of protein) was solubilized with 10 mM phosphate buffer, pH 7.4, containing 20% glycerol, 0.5% sodium cholate, 0.5 M NaCl, and 0.1 mM EDTA, loaded onto a 15 mL octyl-Sepharose column, and eluted with 0.5% Triton X-100. Detergents were removed by loading the proteins on a 1g hydroxyapatite column. CYP 2C9 was eluted with 400 mM phosphate buffer, pH 7.4, 20% glycerol, and 0.1 mM EDTA and appeared to be homogeneous as judged by SDS−PAGE (Coomassie Blue staining) (yield 35%; 15 nmol of P450/mg of protein); purity was also checked by the ratio of absorbance at 417 and 280 nm, which was never less than 1. P450 concentrations were determined according to the method of Omura and Sato (1964).

Cytochrome P450 reductase was purified from phenobarbital-treated rat liver microsomes using ion-exchange chromatography on a DEAE column, followed by chromatography on adenosine 2′,5′-diphosphate−agarose and elution with 2′-AMP; fractions containing reductase activity were concentrated and dialyzed against 100 mM phosphate buffer, containing 20% glycerol and 0.1 mM EDTA (Yasukochi et al., 1976; Strobel & Dignam, 1978). This protein was found to be homogeneous by SDS−PAGE (Coomassie Blue staining). Its molecular weight appeared to be 75 000, showing no proteolysis of the membrane-anchoring peptide.

Enzymatic Activity Measurements. Hydroxylation of tienilic acid was determined by a spectrophotometric assay (Lopez-Garcia et al., 1993) and covalent binding of tienilic acid metabolites to proteins by precipitation on glass fiber filters as previously described (Dansette et al., 1990). The assay mixtures contained 0.2 μM purified CYP2C9, 0.6 μM purified P450 reductase, 30 μg/mL DLPC, and 100 μM tienilic acid. Reactions were started by addition of 1 mM NADPH.

UV−Visible Spectroscopy. All measurements were done at 27 °C on a Kontron Uvikon 820 dual-beam spectrophotometer.

(A) Binding Constant Determination. The interaction between substrates and purified CYP 2C9 was studied by difference visible spectroscopy (Jefcoate, 1978). Solutions (1 mL) contained 0.4 μM CYP 2C9 in 100 mM phosphate buffer, containing 20% glycerol and 0.1 mM EDTA, pH 7.4. A few microliters aliquots of 1 μM, 10 μM, 100 μM, 1 mM, and 10 mM solutions of the substrate in water were added to the sample cuvette, and the same volume of water was added to the reference cuvette; difference spectra were then recorded. K_D and ΔA_{max} values were calculated by using the Hanes plot ([S]/ΔA vs [S]) (Cornish-Bowden, 1979). Calculations based on the Lineweaver−Burk plot and on nonlinear regression analysis (Kaleidagraph) gave identical K_D values (in the error range).

(B) Spin Shifts Induced by Substrates on CYP 2C9 Containing Sulfaphenazole. Ten microliters of a 1 mM solution of sulfaphenazole was added to a 1 mL solution of 0.4 μM CYP 2C9 to reach a final sulfaphenazole concentration of 10 μM; this concentration is high enough to give

more than 95% conversion of the enzyme to the low-spin form, but it is also low enough to permit displacement of this inhibitor by addition of substrates. Substrates were added to the sample cuvette in order to produce a complete conversion of the enzyme to its high-spin form; the same volume of water was added to the reference cuvette. The amount of high-spin form obtained was calculated by assuming $\Delta\epsilon$ (390-trough) = 126 000 M^{-1} cm^{-1} (Schenkman et al., 1981).

NMR Spectroscopy. Proton NMR measurements were made on a Bruker AMX250 spectrometer operating at 250.13 MHz, internally locked on the ^2H signal of the solvent in a standard 5 mm tube; signals were again referenced to HDO at 4.75 ppm. Studies of the frequency dependence also involved measurements on a Bruker AMX500 operating at 500 MHz. Spectra were acquired and transformed on blocks of 4 K memory. The temperature was kept at 300 K, except for the variable temperature experiments in which it was varied from 278 to 300 K.

Substrates were placed in 500 μL of ^2H_2O, and Tris base was added until solubilization was reached (final substrate concentration 10−40 mM). The pH was then adjusted to 7.4 with ^2HCl. Just before the NMR measurements, enzyme solutions were loaded on a G-25 column to exchange sodium phosphate into Tris-HCl buffer to avoid the formation of substrate sodium salts, which are much less soluble. The enzyme solutions were then treated with Chelex 100 to remove any traces of contaminating metal ions. Samples were not degassed since the contribution of dioxygen was supposed to be constant during the titration.

(A) Measurement of Relaxation Times of Substrate Protons. The ^1H longitudinal relaxation times (T_1) were measured by the standard inversion recovery sequence (180°−τ−90°). A delay of five times the longest T_1 was employed between each sequence, and at least 15 different τ values were used. The value of the longitudinal relaxation time was obtained by a nonlinear least squares fitting of the primary data of the peak height as a function of the delay, τ. T_1 was measured in the initial substrate solution and after each addition to this solution of small amounts (5 μL) of concentrated purified CYP2C9 (30−60 μM). At the end of the titrations, the relaxation times of substrate protons were measured after in situ conversion of CYP2C9 to its diamagnetic ferrous carbonyl complex. In all cases, the final T_{1obs} obtained in the presence of the $Fe^{II}CO$ complex and the T_{1obs} of the initial enzyme−free substrate solution were identical, indicating that no significant paramagnetic contribution possibly due to impurities was involved. These results also showed the lack of any significant diamagnetic or outer-sphere contributions to the observed T_1 due to an interaction with the diamagnetic part of the protein. Complete titrations were performed within 2−3 h. Integrity of CYP2C9 over the course of the experiment was assayed by recording the electronic spectra of its $Fe^{II}CO$ complex at the end of the measurements: no significant formation of P420 could be detected.

(B) Solvent Relaxation Measurements. Samples for measurements of solvent proton relaxation times were prepared by adding a few microliters of a concentrated CYP 2C9 solution to Tris buffer or to a 40 mM tienilic acid solution (1 mL) prepared as described above. The resulting samples were then concentrated to 500 μL in a Centricon 30 apparatus, and the NMR measurements were done. The 500 μL filtrates were used as the buffer or substrate reference samples.

(C) NMR Titrations. Protons of molecules that are bound near a paramagnetic center [here P450 Fe(III)] have their relaxation rates increased by the fluctuating magnetic moment of the electron spin. If molecules exchange with those in bulk solution, the observed longitudinal relaxation time will represent the weighted average between the molecules in bulk solution and the ones that are bound to the enzyme (Dwek, 1973; Mildvan & Gupta, 1978). This condition is usually met when a large amount of substrate relative to the enzyme is used; in this case

$$\frac{1}{T_{1obs}} = \left(\frac{1}{T_{1b}} - \frac{1}{T_{1f}}\right)\frac{E_0}{K_D + S_0} + \frac{1}{T_{1f}} \quad (1)$$

where T_{1obs} is the observed relaxation time for a given proton, T_{1b} is the relaxation time of the bound substrate, T_{1f} is the relaxation time for the free substrate, K_D is the dissociation constant of the enzyme−substrate complex, and E_0 and S_0 are the total enzyme and substrate concentrations, respectively. In the presence of a large excess of substrate, which is used in our experiments, the enzyme is almost entirely bound to the substrate (see Results for confirmation of that point). For solvent relaxation all the theory explained above is still applicable, but while we consider a 1:1 stoichiometry for the enzyme−substrate complex, one must consider the number of exchangeable protons in the coordination sphere of the metal in the case of the solvent (Mildvan & Gupta, 1978). In that case, eq 1 becomes

$$\frac{1}{T_{1obs}} = \left(\frac{1}{T_{1b}} - \frac{1}{T_{1f}}\right)\frac{E_0}{K_D + nS_0} + \frac{1}{T_{1f}} \quad (2)$$

The slope of a plot of T_{1obs}^{-1} vs $E_0/(K_D + S_0)$ or T_{1obs}^{-1} vs $E_0/(K_D + nS_0)$ gives the value of T_{1b}, which is correlated to the paramagnetic relaxation time (T_{1M}) by the equation (Dwek, 1973):

$$T_{1b} = T_{1M} + \tau_m \quad (3)$$

where τ_m is the residence time of the substrate in the enzyme active site.

Even if the substrate is in fast exchange between the bound and free forms, so that only one averaged signal is observed, exchange limitations due to τ_m can alter the value of T_{1M}. In the case of the CYP 2C9 substrates used in this study which exhibit K_D values in the 1−100 μM range, τ_m values greater than 10^{-4} s seem unlikely (Banci et al., 1994); thus, eq 3 can be simplied to

$$T_{1b} = T_{1M} \quad (4)$$

In order to verify this approximation, experiments were done on the temperature dependence of T_{1b}; they are based on the fact that T_{1M} and τ_m have opposite temperature dependences. A negative or small positive activation energy for T_{1b} indicates that it is dominated by the paramagnetic contribution T_{1M}, while a large positive activation energy indicates the preponderance of a rate constant, τ_m, which follows an Arrhenius equation (Dwek, 1973; Bertini et al., 1986).

(D) NMR Data Analysis. The effect of the electron spin relaxation on the longitudinal relaxation times is described

by the Solomon−Bloembergen equation (Solomon, 1955; Solomon & Bloembergen, 1956; Bloembergen, 1957):

$$\frac{1}{T_{1M}} = \frac{2h^2\gamma_I{}^2\gamma_S{}^2S(S+1)}{15r^6}\left[\frac{3\tau_c}{1+\omega_I{}^2\tau_c{}^2}+\frac{7\tau_c}{1+\omega_S{}^2\tau_c{}^2}\right]+\frac{2}{3}\frac{S(S+1)A^2}{h^2}\left[\frac{\tau_e}{1+\omega_S{}^2\tau_e{}^2}\right] \quad (5)$$

γ_I and γ_S are respectively the nuclear and electron giromagnetic ratio, h is the reduced Planck constant, S is the total electron spin, τ_c is the correlation time which describes the process which modulates the electron−nuclear dipolar coupling, and ω_I and ω_S are the proton and electron Larmor frequencies, respectively. The first term of eq 5 describes the dipolar interaction; the second one corresponds to the contact interaction which is always negligible since for the proton A/h < 1MHz (Swift & Connick, 1962). The correlation time τ_c is given by

$$\tau_c{}^{-1} = \tau_r{}^{-1} + \tau_S{}^{-1} + \tau_m{}^{-1} \quad (6)$$

where τ_r is the rotational correlation time, τ_s is the electron spin relaxation time, and τ_m is the time for the chemical exchange (Bertini et al., 1986). The fastest process in solution will contribute to τ_c most significantly. In the case of hemoproteins

$$\tau_c = \tau_s \quad (7)$$

τ_s is in the order of 10^{-11}−10^{-10} s for high- and low-spin ferric hemoproteins (Bertini et al., 1986).

(E) τ_s Measurements. Many ways of calculating τ_s have been proposed. We chose to estimate it by the frequency dependence of the relaxation rates (Modi et al., 1995). The paramagnetic relaxation rate is frequency dependent if the τ_c value is comparable to ω_I, so one can estimate τ_s from a plot of T_{1M} vs the frequency. Of course, τ_s must not have a frequency dependence, which is the case for P450s. τ_s measurements are not that precise but owing to the presence of r^6 in eq 5, a difference of 1 order of magnitude in the estimation of τ_s would give a difference of 20% in the distances, but this changes all the absolute values of the distances by a constant factor, not influencing the relative distances for protons in the same molecule. Experimental error associated with the distance estimates was calculated using a method for the propagation of the error through a nonlinear equation (Shoemaker et al., 1974). The error with respect to r was determined by partial derivatives of the Solomon−Bloembergen equations with respect to the relaxation rate variable.

(F) Computer-Assisted Molecular Modeling. Molecular modeling studies were carried out on an IRIS 4D/25 Silicon Graphics workstation. The initial geometries of the molecules were taken from the Cambridge Structural Database (Allen et al., 1993) (REFCODES = SIKLIH, TIENLC, LAURAC, FIXNUV) or were, when necessary, interactively built using the routines of the InsightII module from MSI. Energy minimization was done using the Discover molecular simulation program version 2.96 from MSI (force field, cvff 3.0; minimizer, conjugate gradient; maximum derivative, 0.001 kcal/mol). Partial atomic charges were then calculated using the semiempirical MNDO method version 2.10 (MOPAC). For each molecule, a conformation compatible with the NMR results was then determined by using the MSI package tools which involve (i) the definition of a set consisting of the molecule and an uncharged dummy atom (playing the role of the iron atom) and (ii) energy minimization of this set, using Discover, under the constraint of the NMR distances between the dummy atom (iron) and substrate protons (method, conjugate gradient; maximum derivative, 0.001 kcal/mol). The highest energy difference allowed between the target conformation and the lowest energy conformation was set to 5 kcal (extended to 8 kcal for tienilic acid phenol). Moreover, the differences between the final iron−proton distances obtained after energy minimization and the estimated distances were not allowed to be higher than the experimental errors. For lauric acid, a flexible molecule, an additional distance constraint was applied: the distance between the hydroxylation site and the carboxylate was loosely constrained to the average value which was measured from the other more rigid molecules. Superimposing the molecules was performed using a gradual approach, starting with the most rigid molecules. Initially, three positions were superimposed: the iron atom, the geometrical centroid of the hydroxylation site atoms, and the geometrical centroid of the negatively charged atoms of substrates. Superimposing was then gradually optimized by subsequent flexible fitting procedures allowing low-energy modification of side chains.

RESULTS

Purification of CYP 2C9. Recombinant CYP 2C9 was obtained from expression of the corresponding cDNA (MP-4 clone; Umbenhauer et al., 1987) in yeast strain W(R) fur1 in which yeast cytochrome P450 reductase was overexpressed (Truan et al., 1993). The CYP 2C9 content of yeast microsomes was 130 pmol of P450/mg of protein. Purification with classical techniques previously used for P450s (Imai, 1976) led to very pure CYP 2C9 (≃30% yield) as shown in Figure 1, which presents the SDS−polyacrylamide gel electrophoresis analysis at each step of the purification procedure. The UV−visible spectrum of purified CYP 2C9 is typical of a P450, with a Soret peak at 417 nm and α and β bands a 533 and 568 nm, while the spectrum of the Fe^{II}-CO complex exhibits peaks at 450 and 552 nm (Figure 2). In the presence of cytochrome P450 reductase (purified from rat liver) and dilauroylphosphatidylcholine (DLPC), purified CYP 2C9 catalyzed the 5-hydroxylation of tienilic acid by NADPH and O_2; its activity (2.4 nmol of product (nmol of P450)$^{-1}$ min^{-1}) was very similar to the one reported for yeast microsomes expressing CYP 2C9 (2.02 ± 0.02) (Lopez-Garcia et al., 1993). Moreover, this CYP 2C9-based reconstituted system also reproduced quite well the covalent binding of tienilic acid metabolites to proteins [about 1 nmol (nmol of P450)$^{-1}$ in the presence of glutathione], which was found to be responsible for enzyme inactivation (Lopez-Garcia et al., 1994).

Interaction of Substrates with CYP 2C9. Addition of various substrates, such as tienilic acid (TA), its isomer (TAI), the phenol derived from tienilic acid by loss of its CH_2COOH function (called tienilic acid phenol in the following tables and figures), lauric acid, and diclofenac (formula shown in Figure 4), to purified CYP 2C9 led to a decrease of its Soret peak at 417 nm and to an increase of a band at 390 nm. This is typical of a change of the spin

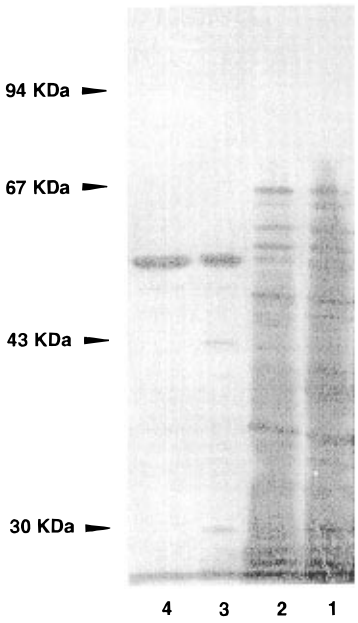

FIGURE 1: Purification of CYP 2C9: SDS-polyacrylamide gel electrophoresis of CYP 2C9 fractions following each purification step. Samples were electrophoresed according to Laemmli (1970) using a 9% (w/v) acrylamide concentration. The gel was transferred on a PVDF membrane for 1 h at 15 V, and the membrane was stained with Coomassie Blue. One microgram of CYP 2C9 was present in each electrophoresed sample. Lanes 1, solubilized yeast microsomes; 2, octyl-Sepharose 4B column eluate during loading of the solubilized microsomes; 3, octyl-Sepharose 4B column fraction after elution with 0.5% Triton X-100; 4, fraction obtained from the hydroxylapatite column.

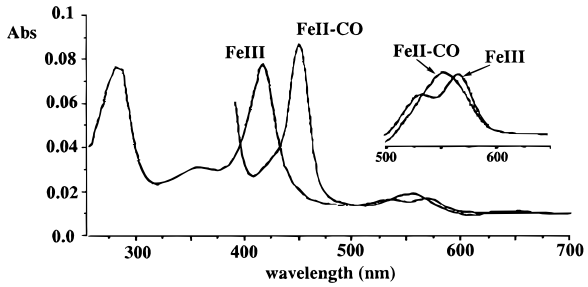

FIGURE 2: Absolute UV−visible spectra of purified recombinant CYP 2C9 and its Fe(II)−CO complex at 20 °C. CYP 2C9 Fe(III) was 0.67 μM in 0.1 M phosphate buffer, pH 7.4, containing 20% glycerol. The CYP2C9 Fe(II)−CO complex was obtained by bubbling CO in the sample cuvette after addition of dithionite.

state of the heme iron from low spin ($S = {}^1/_2$) to high spin ($S = {}^5/_2$), which is due to the binding of the substrate to the protein in close proximity of the heme (type I interaction) (Dawson, 1988). The dependence of these changes on the concentration of substrates (see Figure 3 in the case of the tienilic acid isomer) was used to calculate the equilibrium constant for substrate binding. Table 1 shows that the equilibrium dissociation constants, K_D, for the CYP 2C9−substrate complexes varied between 1.2 μM for TAI and 42 μM for lauric acid at 27 °C. The values for maximal spectral changes, ΔA_{max} (390−417 nm), corresponded to 60−70% spin-state conversion at saturating substrate concentrations under those conditions (Table 1). Addition of sulfaphenazole to CYP 2C9 had an opposite effect as it led to the appearance of a 425 nm peak (Table 1). This corresponds to the binding of its NH_2 group to CYP 2C9 Fe(III) (type II interaction) (Mancy et al., 1996) and to a high-spin to low-spin state

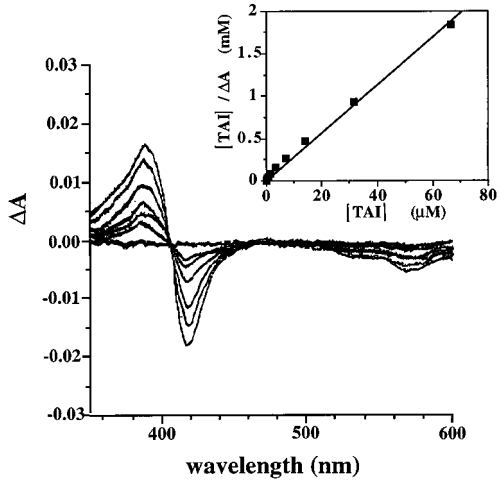

FIGURE 3: Difference UV−visible spectra obtained upon addition of the tienilic acid isomer to purified CYP 2C9 at 27 °C. Both cuvettes contained 0.4 μM CYP 2C9 in 0.1 M phosphate buffer, pH 7.4, containing 20% glycerol. The indicated spectra were obtained after addition of TAI to the sample cuvette in order to reach 0.07, 0.7, 7, 14, 32, and 67 μM concentrations. Insert: Hanes plot of [TAI]/DA (390−417 nm) vs [TAI] used to calculate K_D.

Table 1: Spectral Characteristics of the Binding of Various Substrates to Purified CYP 2C9 at 27 °C[a]

substrate	spectrum type, $\lambda_{max-min}$ (nm)	K_D (μM)	$\Delta\epsilon_{peak\ to\ trough}$ ($M^{-1}\ cm^{-1}$)	% spin change
tienilic acid	I (390−417)	1.4	79 700	64
tienilic acid isomer	I (390−417)	1.2	91 000	72
lauric acid	I (390−417)	42	76 000	61
diclofenac	I (390−417)	25	76 300	61
sulfaphenazole	II (425−390)	0.6	30 000	23

[a] The two cuvettes contained 0.4 μM CYP 2C9 in 0.1 M phosphate buffer, pH 7.4, with 20% glycerol. Difference spectra were obtained after addition of increasing concentrations of substrates in the sample cuvette. The intensities of spectral changes at substrate saturation, $\Delta\epsilon$, and dissociation constants of the CYP 2C9−substrate complexes, K_D, were calculated from the Hanes plot of [substrate]/ΔA versus [substrate]. Percent spin changes were calculated from $\Delta\epsilon_{(peak-trough)} = 126\ 000\ M^{-1}\ cm^{-1}$ (Schenkman et al., 1981).

Table 2: Spin Change of CYP 2C9 in the Presence of Sulfaphenazole upon Addition of Various Substrates at 27 °C[a]

substrate	$\lambda_{max-min}$ (nm)	$\Delta\epsilon_{390-425}$ ($M^{-1}\ cm^{-1}$)	% spin change
tienilic acid	390−425	118 000	94
tienilic acid isomer	390−425	120 000	96
lauric acid	390−425	100 000	79
diclofenac	390−425	107 000	85

[a] The two cuvettes contained 0.4 μM purified CYP 2C9 (conditions as in Table 1) and 10 μM sulfaphenazole. Difference visible spectra were recorded after addition of large concentrations of substrates (2 mM). Percent spin change was calculated as in Table 1.

change. Further addition of saturating amounts of type I substrates, such as tienilic acid, to CYP 2C9 treated with sulfaphenazole that was entirely low spin, led to type I spectra corresponding to conversions to high-spin CYP 2C9 between 79% and 96% (Table 2). Calculations based on the K_D of substrates and sulfaphenazole led to very similar conversion values. This clearly indicates that all the substrates used in the following ^1H NMR study completely convert P450 2C9 into high-spin enzyme−substrate complexes at 27 °C. This is a very important property for calculation of iron−substrate proton distances from para-

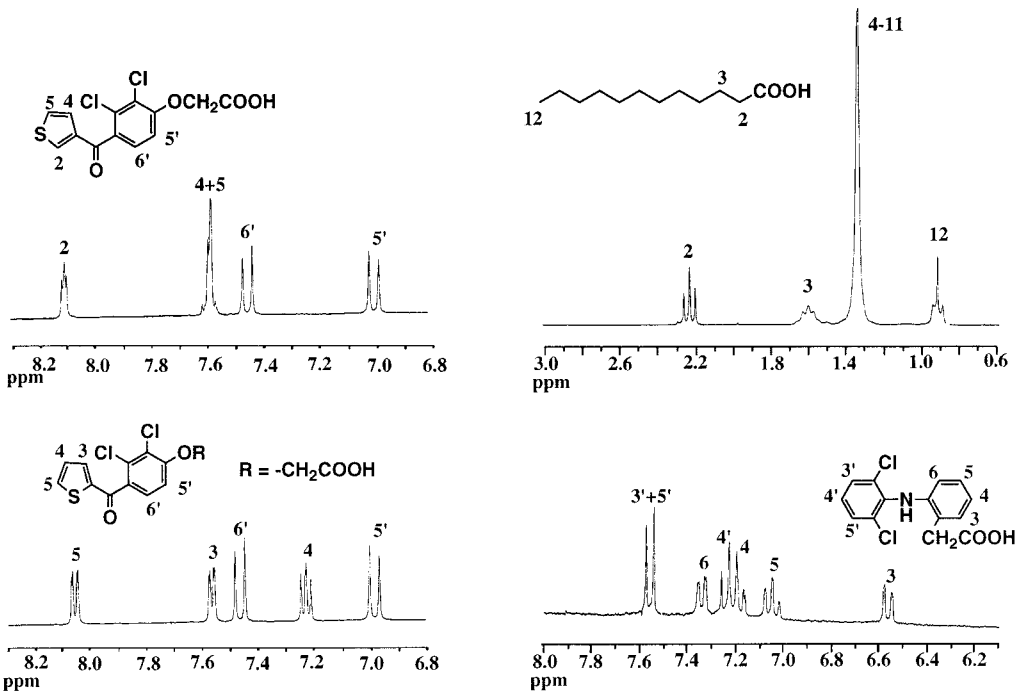

FIGURE 4: ^{1}H NMR spectra of CYP 2C9 substrates at 27 °C. All solutions were made in deuterated Tris buffer (concentration double that of substrate), pH 7.4, prepared as reported in Materials and Methods. Tienilic acid, its isomer, and tienilic acid phenol were 40 mM and lauric acid and diclofenac 10 mM. The proton resonance assignments are indicated on the spectra. The spectrum of tienilic acid phenol (R = OH) is very similar to that of TA; it is not shown.

magnetic relaxation measurements (see following paragraphs).

^{1}H NMR Study of CYP 2C9−Substrate Complexes. Calculation of the paramagnetic relaxation effects of the heme iron on substrate protons in order to determine distances between individual protons of the bound substrate and P450 iron by using the Solomon−Bloembergen equation (eq 5 of Materials and Methods) as described previously for other P450s (Novak & Vatsis, 1982; Modi et al., 1995, 1996), requires (a) the knowledge of the spin state of the enzyme−substrate complex under the conditions of the NMR experiments, (b) the value of the dissociation constant of the enzyme−substrate complex, (c) the value of τ_c, the correlation time of the dipolar interaction between the nuclear and the total electron spin, *S*, and (d) proof that the substrate is exchanging rapidly, relative to the longitudinal relaxation rate, between the active site and the bulk solution. The aforementioned data from UV−visible studies of interactions between purified CYP 2C9 and substrates at 27 °C, the temperature used for the NMR study, answered to points a and b. They showed that saturating concentrations of TA, TAI, tienilic acid phenol, lauric acid, and diclofenac completely convert CYP 2C9 to high-spin ($S = {}^5/_2$) enzyme−substrate complexes; the K_D values of those complexes are shown in Table 1.

Answers to points c and d came from ^{1}H NMR measurements as follows. The ^{1}H NMR spectra of the substrates studied are presented in Figure 4. Resonance assignments are given in the figure. Resonances upfield to that of H_2O that belong to $-CH_2-$ of side chains on aromatic rings have not been studied because CYP 2C9 was added in a solution containing Tris and glycerol which obscured this region of the spectra. The ^{1}H NMR spectrum of TA consists of well-resolved signals which can be easily followed during the experiment. Tienilic acid phenol shows an identical signal pattern spectrum, with slightly different chemical shifts; its spectrum was not shown. The spectrum of TAI is less well resolved, and protons 4 and 5 on the thiophene ring are isochronous. T_1 measurements did not allow us to obtain different values for these two protons, indicating that their distances to iron are very similar. All the other protons could be easily identified. The spectrum of laurate is poorly resolved. Only protons at C2, C3, and C12, which represent important positions in the molecule, could be identified and followed. The spectrum of diclofenac is more complicated. The resonance assignments shown were obtained by a standard decoupling sequence. In diclofenac, protons 4 and 4′ are the most difficult to study, since they overlap in part. Choosing the extreme signals of the multiplet, it was possible to have at least an estimate for the distances of proton 4′ from the iron center.

The longitudinal relaxation times were measured for each assigned proton in the presence of increasing amounts of CYP2C9. The observed dependence of the longitudinal relaxation times for all the protons upon increasing the amount of bound substrate was indicative of an interaction of the substrate with the paramagnetic center. Any diamagnetic contribution was excluded since the relaxation times observed for the substrates alone in the buffer were unchanged after addition of diamagnetic CYP 2C9−Fe^{II}CO (data not shown).

A typical plot of the observed relaxation rates (T_{1obs}) as a function of substrate-bound fraction for all the resonances of TA, TAI, and diclofenac is shown in Figure 5. The straight lines obtained and the different slopes observed for different protons of the same molecule were a first hint that the substrates are in fast chemical exchange relative to the paramagnetic relaxation rates (Dwek, 1973; Bertini et al., 1986). Such straight lines were obtained for all the substrates used in this study. Demonstration that fast exchange of the substrates occurred in our conditions was obtained from a study of the temperature dependence of the relaxation times

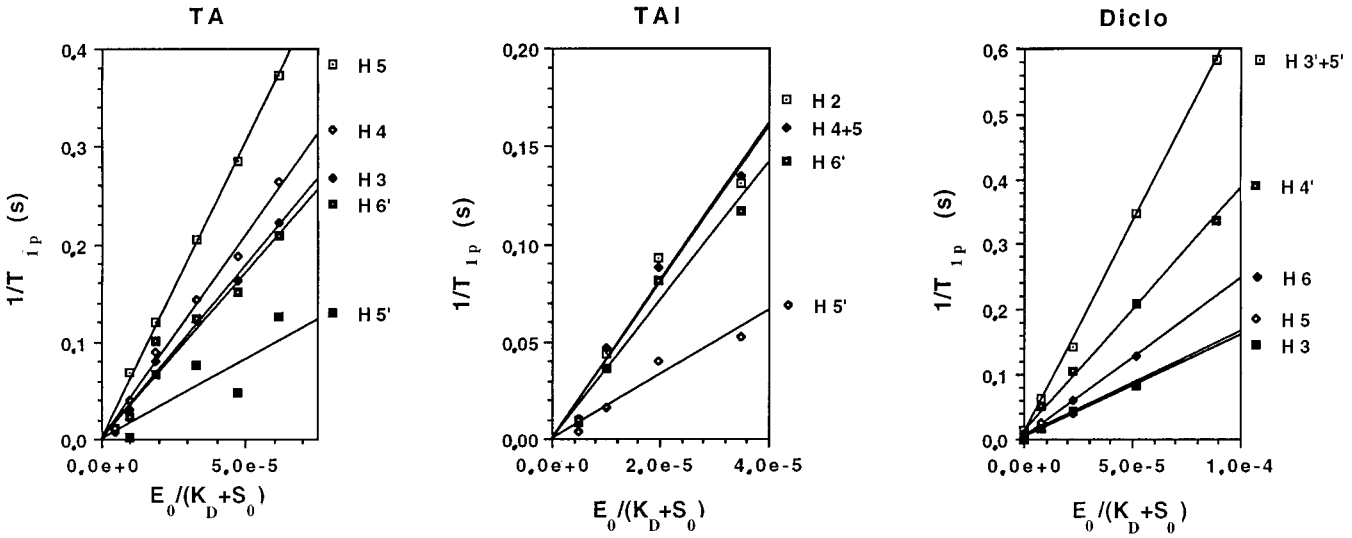

FIGURE 5: Effects of CYP 2C9 on the longitudinal relaxation rates of substrate protons. T_{1obs} values were measured after addition of increasing amounts of purified CYP 2C9 (concentration = E_0, from 0 to 5 μM) to a solution of substrates (TA, TAI, and diclofenac) in deuterated Tris buffer, pH 7.4 (substrate concentration = S_0). Final concentrations of glycerol coming from enzyme purification were less than 0.1%. Figures are plots of $1/T_{1p}$ vs $E_0/(K_D + S_0)$, where $1/T_{1p} = 1/T_{1obs} - 1/T_{1f}$. As explained in Materials and Methods (eq 2), the slope of the lines gives the value for $1/T_{1M}$ reported in Table 3.

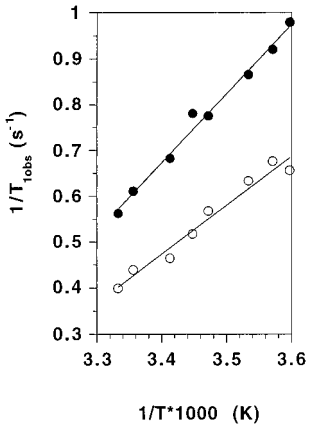

FIGURE 6: Temperature dependence of the longitudinal relaxation time of the NMR resonance of tienilic acid proton 5. Measurements were made at 250 MHz with 40 mM substrate in the absence of CYP 2C9 (open circles) and in the presence of 4 μM CYP 2C9 (filled circles) in deuterated Tris buffer, pH 7.4.

of TA protons at fixed TA and CYP 2C9 concentrations. The Arrhenius plot depicting this temperature dependence of the relaxation rates of the TA proton that is the nearest to the iron (H_5) is shown in Figure 6. This plot yields a negative activation energy of -4 kcal/mol for the relaxation rate of that proton in the bound substrate. The values determined for the other protons of TA were all negative, and a mean value of -9 ± 5 kcal/mol was estimated for the molecule. These data clearly confirmed that T_{1b} is independent from τ_m (Novak & Vatsis, 1982). Results showing a linear dependence of the proton relaxation times as a function of temperature were obtained for all the other substrates used in this study.

Estimation of the correlation time of the electron spin relaxation τ_c ($=\tau_s$; see Materials and Methods) was made by measuring the H_2O protons' relaxation rate in the presence of CYP 2C9 at 250 and 500 MHz. This gave a value of 2×10^{-10} s, which is an approximation well in the range of previously estimated τ_s values for other P450s (Griffin & Peterson, 1975; Philson et al., 1979; Woldman et al., 1985; Modi et al., 1995), and very similar to that recently reported for another human liver P450, P450 2D6 (Modi et al., 1996). The fact that a water molecule is present or not on the coordination sphere of the iron when the substrate is present has been studied by the NMR measurements of the relaxation times of water on the free and tienilic acid bound CYP 2C9. In this case the iron−water proton distance changes from 2.4 to 3.6 Å.

Finally, iron−substrate proton distances were calculated from the T_{1M} values determined for each proton of the various compounds studied that gave a type I interaction with CYP 2C9 (TA, TAI, TA phenol, lauric acid, and diclofenac) as explained in Materials and Methods (Table 3).

In the particular case of sulfaphenazole, similar NMR measurements after addition of CYP 2C9 only showed a small but significant paramagnetic effect on the protons ortho to the NH_2 group of the aniline part of the molecule (data not shown). Such a small effect is not surprising since sulfaphenazole was found to bind to the CYP 2C9 iron(III) leading to a low-spin ($S = {}^1/_2$) CYP 2C9 complex (Table 1) (Mancy et al., 1996). Paramagnetic effects caused by low-spin Fe(III) are much smaller than those induced by high-spin Fe(III) centers and are generally not easily observed (Bertini et al., 1986). The small paramagnetic effect selectively observed on the aniline ortho protons of sulfaphenazole should derive from their close proximity to the CYP 2C9 iron that is due to sulfaphenazole binding via its NH_2 function. This result is in agreement with recent biochemical results on the nature of CYP 2C9−sulfaphenazole interactions (Figure 8) (Mancy et al., 1996).

Position of Substrates Relative to CYP 2C9 Iron Based on NMR Data and Molecular Modeling. For each substrate studied, a 3D model consisting of the substrate plus iron (defined as a dummy atom) that corresponds to the iron−proton distances of Table 3 was built. Starting conformations of the substrates used for constructing this model were either drawn from X-ray crystallographic data or deduced from energy minimization calculations (Mancy et al., 1995). The energy of substrate conformations finally found in those models compatible with NMR distances and the associated errors was never higher than 5 kcal/mol, except for tienilic

Table 3: Paramagnetic Relaxation Times of the Protons of Substrates Bound to CYP 2C9 and Corresponding Calculated Iron−Proton Distances[a]

		proton					
substrate	parameter	**2**	**3**	**4**	**5**	**5′**	**6′**
tienilic acid	T_{1M} (μs)		281 ± 20	240 ± 24	165 ± 7	616 ± 226	294 ± 60
	r (Å)		5.9 ± 0.1	5.8 ± 0.1	5.4 ± 0.05	6.7 ± 0.4	6.0 ± 0.2
tienilic acid isomer	T_{1M} (μs)	250 ± 38		247 ± 29[b]	247 ± 29[b]	611 ± 114	283 ± 39
	r (Å)	5.8 ± 0.15		5.8 ± 0.1	5.8 ± 0.1	6.7 ± 0.2	5.9 ± 0.2
tienilic acid phenol	T_{1M} (μs)		124 ± 5.5	114 ± 7	107 ± 7	131 ± 20	145 ± 8
	r (Å)		5.2 ± 0.04	5.2 ± 0.05	5.1 ± 0.05	5.3 ± 0.15	5.4 ± 0.05

		proton			
substrate	parameter	**2**	**3**	**4−11**	**12**
lauric acid	T_{1M} (μs)	542 ± 44	488 ± 11	296 ± 44	524 ± 17
	r (Å)	6.6 ± 0.1	6.5 ± 0.05	6.0 ± 0.1	6.6 ± 0.05

		proton					
substrate	parameter	**3**	**4**	**5**	**6**	**3′(5′)**	**4′**
diclofenac	T_{1M} (μs)	635 ± 33	nd[c]	619 ± 63	410 ± 25	155 ± 4.5	269 ± 11
	r (Å)	6.9 ± 0.06	nd[c]	6.9 ± 0.1	6.4 ± 0.07	5.4 ± 0.02	6.0 ± 0.04

[a] Conditions of Figure 5 and calculations indicated in Materials and Methods. [b] Isochronous protons. [c] Not determined.

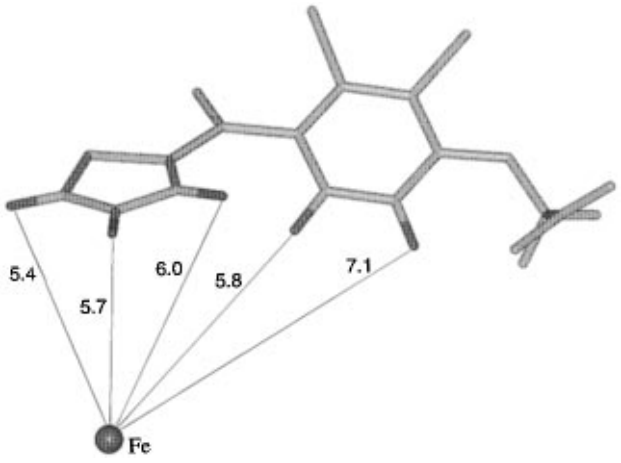

FIGURE 7: Positioning of tienilic acid relative to the heme iron according to the iron−proton distances listed in Table 3. Protons for which distances to iron were estimated are in black. Distances found after energy minimization under NMR distance constraints are in angstroms.

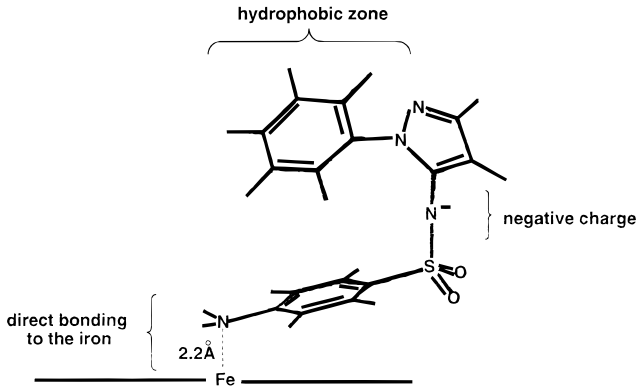

FIGURE 8: Formula and mode of binding of sulfaphenazole to CYP 2C9 iron [according to Mancy et al. (1996)].

acid phenol (8 kcal). The model found for the tienilic acid−iron set is shown in Figure 7, as an illustration. Then, the substrate−iron models were superimposed with the following constraints: (i) superposition of the irons, (ii) close positioning of the known hydroxylation sites of the substrates [substrate hydroxylation sites as indicated in Mancy et al. (1995), except for lauric acid which was found to be mainly hydroxylated at the ω-1 position by CYP 2C9; Boucher et al., in preparation], and (iii) close positioning of the anionic atoms of the substrates. Superimposition of the substrates was then gradually optimized by subsequent flexible fitting procedures allowing low-energy changes of side chains. In the final model shown in Figure 9, all the hydroxylation sites of the substrates are very close and located about 5 Å from the iron. The substrate anionic sites (carboxylate or phenol oxygen atoms) are all within a 4 ± 0.5 Å distance from a common point in the space which could be a cationic site of the protein; these distances are compatible with an ionic interaction between the substrate anionic site and the protein cationic residue (Mancy et al., 1995).

Finally, sulfaphenazole was incorporated in the model, the two conformations found in the corresponding X-ray structure (Patel & Singh, 1987) being used initially. Its NH_2 nitrogen atom was positioned in order to establish a bond with CYP 2C9−iron, i.e., with a proper orientation of its nitrogen lone pair toward iron. An Fe−N distance of 2.2 Å, a classical value for (porphyrin)iron−nitrogen distances in iron−primary amine complexes (Mansuy et al., 1983), was chosen. Then, a positioning for both conformations leading to such a Fe−N bond was found in which the N^- anionic site of sulfaphenazole was located at a distance from the protein cationic site compatible with an ionic bond (3.7 Å). In one of the two starting conformations, the *N*-phenyl group of sulfaphenazole is very well located in a hydrophobic region of the CYP 2C9 substrate envelope; for instance, it is close to the dichlorophenyl groups of the tienilic acid derivatives. The presence of a hydrophobic group on the pyrazole nitrogen atom of sulfaphenazole has been found to be crucial for the strong inhibitory effects of this compound (Mancy et al., 1996).

DISCUSSION

In the model previously proposed for the interaction of CYP 2C9 with its substrates (Mancy et al., 1995), the pharmacophore recognized by CYP 2C9 corresponded to an

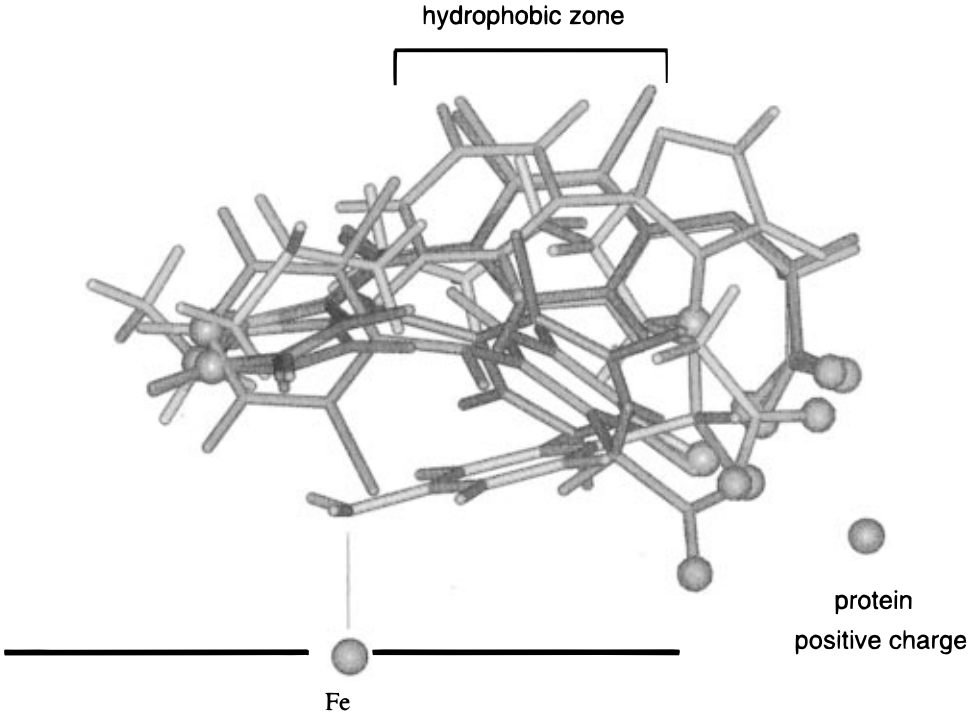

FIGURE 9: Possible positioning of various substrates and sulfaphenazole in the active site of CYP 2C9. This model was obtained by superimposing the various iron-substrate sets similar to that of Figure 7. The hydroxylation sites of all substrates are almost superimposed and appear on the left as gray balls. The anionic atoms of the substrates appear on the right as gray balls; they are all within 4.0 ± 0.5 Å from a putative cationic site of the protein (golden spot). The heme iron is shown as a purple spot. TA, TAI, tienilic acid phenol, lauric acid, and diclofenac are shown in dark blue, light blue, green, yellow, and red, respectively. Sulfaphenazole (in magenta) was incorporated in the model by taking into account its binding to iron via its NH_2 function and the interaction of its N^- site with the protein cationic site.

envelope of 12 substrates which all exhibit an anionic site about 8 Å distant from their hydroxylation site by CYP 2C9. It was not possible to determine the iron−substrate proton distances for all of those substrates from NMR measurements, as some substrates such as phenytoin were not soluble enough at pH 7.4, and others, such as piroxicam and tenoxicam, did not involve significant paramagnetic effects upon titration with CYP 2C9. The latter phenomenon should be due to the formation of low-spin iron(III) complexes between piroxicam (and tenoxicam) and CYP 2C9, possibly due to the binding of their pyridine nitrogen atom to iron, instead of the formation of high-spin CYP 2C9−substrate (type I) complexes. Unfortunately, this hypothesis could not be confirmed by visible spectroscopy because of a strong absorption of those two substrates in the 400 nm region.

However, iron−proton distances could be easily calculated for five type I substrates, TA, TAI, tienilic acid phenol, lauric acid, and diclofenac, as the addition of CYP 2C9 to those substrates caused a strong decrease of the relaxation times of their protons. Upon substrate binding to P450s a variable number of water molecules are usually expelled from the active site including the one which coordinates to the heme iron (Poulos et al., 1987; Raag & Poulos, 1991; Jacobs et al., 1987). In some cases, a few water molecules may remain in the active site. NMR measurements of the paramagnetic contribution to the relaxation rate of the solvent protons give the distance of the nearest exchangeable proton from the paramagnetic center. Assuming that two protons belonging to a water molecule rapidly exchange, we estimated a water proton−iron distance of 2.4 Å (calculated using a τ_c value obtained as described above) for CYP 2C9 in the absence of substrate, which is in agreement with the previously measured distances for P450 BM3 (2.6 Å; Modi et al., 1995), P450 cam (2.6 Å; Philson et al., 1979), and P450 scc (2.7 Å; Jacobs et al., 1987) and with the distance observed, for instance, in the crystal structure of P450 BM3 (2.28 Å; Ravichandran et al., 1993). This distance is short enough to account for a directly bound water molecule as an axial ligand to the heme. Upon addition of tienilic acid to CYP 2C9, the distance that we calculated was longer (3.5 Å) but suggested that a proton remains significantly close to the iron as happens in P-450 scc upon binding of cholesterol (3.9 Å; Jacobs et al., 1987). This indicates that an exchangeable proton (from water or an amino acid side chain) is still present near the iron (Raag & Poulos, 1991) and that the active site is probably still accessible to water. A more complete study on the displacement of water induced by other substrates would be useful to clear this point, but such a study is beyond our objectives.

The final model of Figure 9 is based on the iron−substrate proton distances calculated from the NMR experiments (Table 3). It is noteworthy that those distances could represent the time-averaged orientation of the substrate in the CYP 2C9 active site if this substrate can adopt different conformations or positions in the active site. There is presently no way of experimentally distinguishing this situation from a situation in which the substrate is fixed in the active site. However, the specific ability of CYP 2C9 to recognize substrates involving an anionic site and to hydroxylate them at another site about 8 Å distant from the anionic one strongly suggests that those anionic substrates are preferentially bound in only one conformation. Anyway, NMR and molecular modeling results depicted in Figure 9 are in good agreement with previously reported data. For instance, the distances found between the iron atom and the hydroxylation site were about 5 Å for all substrates. In the

X-ray structure of the P450 cam−camphor complex, this distance is 4 Å (Poulos et al., 1987), and NMR measurements performed on other P450s gave values between 5 and 7 Å (Novak et al., 1982; Woldman et al., 1993; Van der Straat et al., 1987). The value found for CYP 2C9 is thus comparable to those obtained for other P450s. In that regard, it is noterworthy that the distances calculated from NMR relaxation experiments are dependent on the value used for the correlation time τ_s. We found and used a value of 2×10^{-10} s, similar to those previously used for other P450s. If one had used correlation times classical for iron(III) peroxidases and other hemoproteins (5×10^{-11} s; Bertini et al., 1986), a shorter distance close to 4 Å would have been calculated. Anyway, it is noteworthy that the closest approach of substrates to CYP 2C9 iron is about 4−5 Å, whereas exchangeable protons (from water or an amino acid residue of the protein) are closer (3.5 Å) to iron. Such a phenomenon has been observed previously in the case of P450 BM3 (Modi et al., 1995; Li & Poulos, 1996). This would imply that structural changes occurring later in the catalytic cycle of P450 should be required for substrate hydroxylation.

The model of Figure 9 also shows an interesting difference between TA and its isomer TAI. Their thiophene rings are almost superimposed, and position 5 of TA coincides with the sulfur atoms of TAI, whereas position 2 of TAI coincides with the sulfur atom of TA. Position 5 of TA is very important as it is the site of hydroxylation of this drug by CYP 2C9 (Lopez-Garcia et al., 1994), and it is also supposed to be the electrophilic site attacked by a protein nucleophilic group of CYP 2C9 during metabolic activation of TA. This leads to the covalent binding of TA to CYP 2C9 and to the inactivation of this enzyme (Lopez-Garcia et al., 1994). On the contrary, nucleophiles have been found to add on position 2 of TAI sulfoxide, the primary monooxygenation product of TAI by CYP 2C9 (Mansuy et al., 1991). The nucleophilic amino acid residue of CYP 2C9, which is well located in the active site to react at position 5 of TA, should also be close to the sulfur atom of TAI but too far away to react with position 2 of TAI (Figure 9). This would explain the lack of inactivation of CYP 2C9 upon oxidation of TAI (Lopez-Garcia et al., 1994).

Finally, the model presented in Figure 9 is the first positioning of substrates relative to the CYP 2C9 iron that is based on experimentally estimated distances. It underlines that two structural characteristics are important for a substrate (or inhibitor) to be selectively recognized by CYP 2C9: (i) the presence of an anionic site able to establish an ionic bond with a putative cationic residue of the protein and (ii) the presence of a hydrophobic zone between the hydroxylation site and the anionic site, which corresponds to the aryl group of tienilic acid derivatives and the *N*-phenyl group of sulfaphenazole. In the particular case of sulfaphenazole a third structural feature explains its high affinity for CYP 2C9; it is the presence of the NH_2 function well located to establish a bond with the CYP 2C9 iron. The model of Figure 9 will be assessed in a near future by using a CYP 2C9 structure built by homology modeling in order to identify the key amino acid residues responsible for substrate binding.

ACKNOWLEDGMENT

We thank Anphar-Rolland Laboratories (Chilly-Mazarin, France) and Ciba-Geigy (Basel, Switzerland) for providing us with tienilic acid and sulfaphenazole, respectively. One of us (S.P.-S.) thanks Dr. T. Beringhelli (Milan, Italy) for useful discussions.

REFERENCES

Allen, F. H., & Kennard, O. (1993) *Chem. Des. Automation News 8*, 31−37.
Banci, L., Bertini, I., Marconi, S., Pierattelli, R., & Sligar, S. G. (1994) *J. Am. Chem. Soc. 116*, 4866−4873.
Beaune, P. H., Dansette, P. M., Flinois, J. P., Columelli, S., Mansuy, D., & Leroux, J. P. (1979) *Biochem. Biophys. Res. Commun. 88*, 826−832.
Bellamine, A., Gautier, J. C., Urban, P., & Pompon, D. (1994) *Eur. J. Biochem. 225*, 1005−1013.
Bertini, I., & Luchinat, C. (1986) *NMR of Paramagnetic Molecules in Biological Systems*, Chapter 3, The Benjamin Cummings Publishing Co., Inc., New York.
Bloembergen, N. (1957) *J. Chem. Phys. 27*, 572−573.
Cornish-Bowden, A. (1979) *Fundamentals of Enzyme Kinetics*, Chapter 2, pp 25−30, Butterworth & Co., Ltd., New York.
Dansette, P. M., Amar, C., Smith, C., Pons, C., & Mansuy, D. (1990) *Biochem. Pharmacol. 39*, 911−918.
Dawson, J. H. (1988) *Science 248*, 433−439.
Dwek, R. A. (1973) in *NMR in Biochemistry*, pp 11−142, Oxford University Press, London.
Ged, C., Umbenauer, D. R., Bellew, T. M., Bork, R. W., Srivastava, P. K., Shinriki, N., Lloyd, R. S., & Guengerich, F. P. (1988) *Biochemistry 27*, 6929−6940.
Goldstein, J. A., & de Morais, S. M. F. (1994) *Pharmacogenetics 4*, 285−299.
Gonzalez, F. J. (1989) *Pharmacol. Rev. 40*, 243−288.
Griffin, B. W., & Peterson, J. A. (1975) *J. Biol. Chem. 250*, 6445−6451.
Guengerich, F. P., & Turvy, C. G. (1991) *J. Pharmacol. Exp. Ther. 256*, 1189−1194.
Imai, Y. (1976) *J. Biochem. 80*, 267−276.
Jacobs, R. E., Singh, J., & Vickery, L. E. (1987) *Biochemistry 26*, 4541−4545.
Jefcoate, C. R. (1978) *Methods Enzymol. 52*, 258−279.
Jones, B. C., Hawksworth, G., Horne, V. A., Newlands, A. Morsman, J., Tute, M. S., & Smith, D. A. (1996) *Drug Metab. Dispos. 24*, 260−266.
Jones, P. J., He, M., Trager, W. F., & Rettie, A. E. (1996) *Drug Metab. Dispos. 24*, 1−6.
Koerts, J., Rietjens, I. M. C. M., Boersma, M. G., & Vervoort, J. (1995) *FEBS Lett. 368*, 279−284.
Laemmli, U. K. (1970) *Nature 227*, 680−685.
Li, H. Y., & Poulos, T. L. (1996) *Nat. Struct. Biol. 4*, 104−146.
Lopez-Garcia, M. P., Dansette, P. M., Valadon, P., Amar, C., Beaune, P. H., Guengerich, F. P., & Mansuy, D. (1993) *Eur. J. Biochem. 213*, 223−232.
Lopez-Garcia, M. P., Dansette, P. M., & Mansuy, D. (1994) *Biochemistry 33*, 166−175.
Mancy, A., Broto, P., Dijiols, S., Dansette, P. M., & Mansuy, D. (1995) *Biochemistry 34*, 10365−10375.
Mancy, A., Dijols, S., Poli, S., Guengerich, F. P., & Mansuy, D. (1996) *Biochemistry 35*, 16205−16212.
Mansuy, D., Battioni, P., Chottard, J.-C., Riche, C., & Chiaroni, A. (1983) *J. Am. Chem. Soc. 105*, 455−463.
Mansuy, D., Valadon, P., Erdelmeier, I., Lopez-Garcia, P., Amar, C., Girault, J. P., & Dansette, P. (1991) *J. Am. Chem. Soc. 113*, 7825−7826.
Mildvan, A. S., & Gupta, R. K. (1978) *Methods Enzymol. 49*, 322−359.
Modi, S., Primrose, W. U., Boyle, J. M. B., Gibson, C. F., Lian, L. Y., & Roberts, G. C. K. (1995) *Biochemistry 34*, 8982−8988.
Modi, S., Paine, M. J., Sutcliff, M. J., Lian, L.-Y., Primrose, W. U., Wolf, C. R., & Roberts, G. C. K. (1996) *Biochemistry 35*, 4540−4550.
Neau, E., Dansette, P. M., Andronik, V., & Mansuy, D. (1990) *Biochem. Pharmacol. 39*, 1101−1107.
Nelson, D. R., Koymans, L., Kamataki, T., Stegeman, J. J., Feyereisen, R., Waxman, D. J., Waterman, M. R., Gotoh, O.,

Minor, J. C., Estabrook, R. W., Gunsalus, I. C., & Nebert, D. W. (1996) *Pharmacogenetics 6*, 1−42.
Novak, R. F., & Vatsis, K. P. (1982) *Mol. Pharmacol. 21*, 701−709.
Omura, T., & Sato, R. (1964) *J. Biol. Chem. 239*, 2370−2378.
Patel, H. C., & Singh, T. P. (1987) *Acta Crystallogr. C43*, 1131−1134.
Philson, S. B., Debrunner, P. G., Schmidt, P. G., & Gunsalus, I. C. (1979) *J. Biol. Chem. 254*, 10173−10179.
Poulos, T. L., Finzel, B. C., & Howard, A. J. (1987) *J. Mol. Biol. 195*, 687−700.
Raag, R., & Poulos, T. L. (1991) *Biochemistry 30*, 2674−2684.
Ravichandran, K. G., Boddupalli, S. S., Hasemann, C. A., Peterson, J. A., & Deisenhofer, J. (1993) *Science 261*, 731−736.
Romkes, M., Faletto, M. B., Blaisdell, J. A., Raucy, J. L., & Goldstein, J. A. (1991) *Biochemistry 30*, 3247−3255.
Schenkman, J. B., Sligar, S. G., & Cinti, D. L. (1981) *Pharmacol. Ther. 12*, 43−71.
Shoemaker, D. P., Garland, C. W., & Steinfeld, J. I. (1974) in *Experiments in Physical Chemistry*, 3rd ed., pp 52−54, McGraw Hill, New York.
Solomon, I. (1955) *Phys. Rev. 99*, 559−565.
Solomon, I., & Bloembergen, N. (1956) *J. Chem. Phys. 25*, 261−266.
Strobel, H. W., & Dignam, J. D. (1978) *Methods Enzymol. 52*, 89−96.
Swift, T. J., & Connick, R. E. (1962) *J. Chem. Phys. 37*, 307−320.
Truan, G., Cullin, C., Reisdorf, P., Urban, P., & Pompon, D. (1993) *Gene 125*, 49−55.
Umbenhauer, D. R., Martin, M. V., Lloyd, R. S., & Guengerich, F. P. (1987) *Biochemistry 26*, 1094−1099.
Urban, P., Truan, G., Bellamine, A., Laine, R., Gautier, J. C., & Pompon, D. (1994) *Drug Metab. Drug Interact. 11*, 169−200.
Van de Straat, R., De Vires, J., De Boer, H. J. R., Vromans, R. M., & Vermeulen, N. P. E. (1987) *Xenobiotica 17*, 1−9.
Woldman, Y. Y., Weiner, L. M., Gulyaeva, L. F., & Lyakhovich, V. V. (1985) *FEBS Lett. 181*, 295−299.
Woldman, Y. Y., Weiner, L. M., & Lyakhovich, V. V. (1993) *Biochem. Biophys. Res. Commun. 193*, 40−46.
Yasukochi, Y., & Masters, B. S. S. (1976) *J. Biol. Chem. 251*, 5337−5344.

BI970527X